

EXPERIMENTAL TECHNIQUES

Various composition in the systems $\text{BaTi}_{1-x}\text{Sn}_x\text{O}_3$ ($x=0.00, 0.05, 0.15, 0.30$ and 0.40) using barium carbonate, $\text{BaTi}_{1-x}\text{Sn}_x\text{O}_3$ ($x=0.00, 0.10, 0.20, 0.30$ and 0.40) using barium nitrate, Composites $(1-x) \text{BaTi}_{0.85}\text{Sn}_{0.15}\text{O}_3 - (x) \text{NiFe}_2\text{O}_4$ ($x = 5, 10, 15$ and 20 wt.%), $(1-x) \text{BaTi}_{0.85}\text{Sn}_{0.15}\text{O}_3 - (x) \text{CNTs}$ ($x = 5, 10, 15$ and 20 wt.%) and $(1-x) \text{BaTi}_{0.85}\text{Sn}_{0.15}\text{O}_3 - (x) \text{FA}$ (where $x = 5, 10, 15$ and 20 wt.%) have been synthesized by conventional solid state ceramic method. The sample have been charecterized for their thermal properties, crystal structure, microstructural, dielectric and electrical properties. In this chapter detailed mehod of preparation of these materials and the techniques used for their charecterization are described.

2.1 RAW MATERIALS

In the present study, all samples were prepared using analytical reagent grade chemicals.

Different chemicals used for synthesizing these samples are listed in Table 2.1

Table 2.1 Specification of materials used

Raw Materials	Purity	Manufacturer
$\text{Ba}(\text{CO}_3)_2$	99.00%	Aldrich–Sigma, USA
$\text{Ba}(\text{NO}_3)_2$	99.00%	Qualikems, USA
TiO_2	99.50%	Alfa-Aesar, USA
SnO_2	99.90%	Aldrich–Sigma, USA,
$\text{SnCl}_4 \cdot 5\text{H}_2\text{O}$	98.00%	Alfa Aesar ,UK
$\text{Fe}(\text{NO}_3)_3 \cdot 9\text{H}_2\text{O}$	98.00%	Fisher Scientific, India
$\text{Ni}(\text{NO}_3)_2 \cdot 6\text{H}_2\text{O}$	98.00%	Molychem, India
CNTs	--	As prepared

2.2 SYNTHESIS OF MATERIALS

Ceramic materials are one of the major groups in the material science because of their direct and indirect applications in day to day life. Hence the synthesis of new ceramic powders is of great importance in the progress of Material Science. There are several methods of preparation such as mechanical methods which includes solid state reaction, heat sustained method and ball milling, etc., and chemical method which includes sol-gel wet dry and polymer sol-gel, etc. To achieve a good quality with respect to purity, homogeneity, reactivity and particle size, etc., each method finds its own advantages and disadvantages. In this contest solid state reaction and heat sustained method found to be easier, convenient and low-cost technique among other available methods by means of performance, reliability, reproducibility and economy.

2.2.1 Powder and Ceramics of $\text{BaTi}_{1-x}\text{Sn}_x\text{O}_3$

To synthesizing powders and ceramics, we using a stoichiometric amount of raw materials were mixed in a ball mill for 8 h using acetone as the mixing media. The mixed powders were dried in an open atmosphere overnight. Theses mixed powders were calcined at a particular temperature for 12 h. The calcined powders were ground in the agate mortar for two h. All calcined powders were pelletized using a die of 12-mm diameter for 2–3-mm thick pellets. A few drops of 2 % solution of polyvinyl alcohol (PVA) were added to the powders as a binder. Therefore, in this study also pellets were kept in an alumina crucible and sintered at 1350°C. Initially, pellets were heated slowly at a rate of 2°C/min to 200°C. They were maintained at this temperature for 1 h to burn off the binder. After this, pellets were heated at a rate of 5°C/min to the sintering temperature, 1350°C. The pellets were sintered at this temperature for 5 h. After sintering, pellets were cooled with the help of a programmable temperature controller.

A flow chart showing the various steps for the preparation of these materials in different samples is shown in Figure 2.1.

2.2.2 Synthesis of Powder of Ferrite NiFe₂O₄

Stoichiometric amounts of AR grade ferric nitrate [Fe(NO₃)₃·9H₂O] and nickel nitrate [Ni(NO₃)₂·6H₂O] were dissolved in minimum amount of ethylene glycol at room temperature, and the sol was heated at 60°C for two hours to form a wet gel. Thereafter gel was dried at 400°C for approximately 30 minutes; gel self-ignites to form a NiFe₂O₄ powder. The combustion can be considered as a thermally induced redox reaction of the gel wherein ethylene glycol acts as a reducing agent. The nitrate ion provides an in-situ oxidizing environment for the decomposition of the organic component.

2.2.3 Synthesis of Powder of multi-walled carbon nanotube (MW-CNTs)

The synthesis of CNTs by one steps spray pyrolysis techniques using benzene ferrocene as a precursor. The precursor solution is a solution of benzene and ferrocene solution prepared by dissolving the ground powder of ferrocene in benzene with a concentration (30-35 mg/ml). The container of spray pyrolysis was filled with precursor and then precursor sprayed through silica tube which is generally preheated 900⁰C. Through the optimum flow rate, 2ml/min precursor sprayed and the growth of CNTs in the form of a thin film obtained.

2.2.4 Synthesis of Ceramics of Composites and their Constituent Phases

Composites (1-x) BaTi_{0.85}Sn_{0.15}O₃ – (x) NiFe₂O₄(where x = 5, 10, 15 and 20 wt.%), (1-x) BaTi_{0.85}Sn_{0.15}O₃ – (x) CNTs(where x = 5, 10, 15 and 20 wt.%) and (1-x) BaTi_{0.85}Sn_{0.15}O₃ – (x) FA (where x = 5, 10, 15 and 20 wt.%) were obtained by thoroughly mixing the constituent phases BaTi_{0.85}Sn_{0.15}O₃ (BTS) with NiFe₂O₄ (NF) , CNTs and Fly ash (FA) (in desired weight ratios) in a planetary ball mill (Retsch, Germany) for 6 hrs using acetone as a milling medium.

These milled powders and powders of constituent phases were mixed with polyvinyl alcohol (PVA) solution in water, which acts as a binder. The powder mixtures were pressed in the form of pellets of diameter 12 mm and thickness ~ (1.5- 2.0) mm using a stainless- steel die and uniaxial hydraulic press at an optimized load of 50kN. Initially, pellets were heated slowly at a rate of 2°C/min to 200°C and were kept at this temperature for 1 h to burn off the binder. Thereafter, these pellets were sintered for 4h at a rate of 5°C/min. After sintering, pellets were cooled upto at a rate of 5°C/min using programmable temperature controller.

2.2.5 Fly ash Powder

The fly ash powder used in this work was collected from Koradi Thermal Power Station, near Nagpur, India

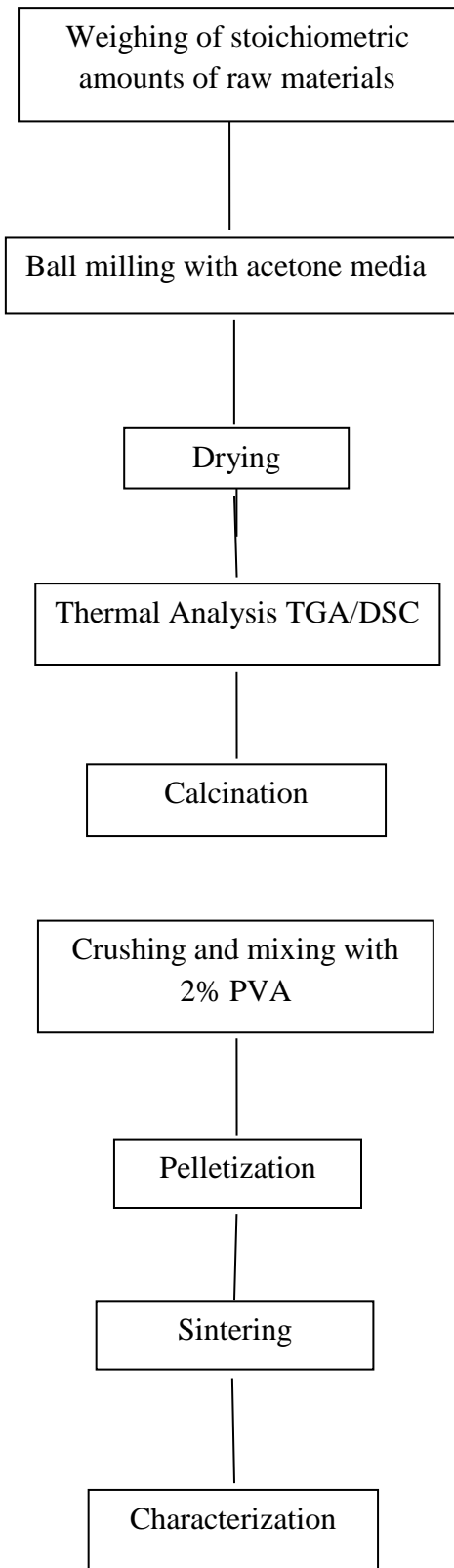


Figure 2.1 Flow chart of synthesis of samples.

2.3 CHARACTERIZATION

2.3.1 Thermal analysis (TG/DSC)

Thermogravimetric analysis (TGA) is a technique used to study the weight change of the material due to evaporation, decomposition and phase change with changing temperature and time under controlled atmosphere [Lei, 2006; Dmitry, 2008]. Hence the requirement of a stable and precise weighing balance becomes very important. The sample is placed in a refractory pan that is positioned in the furnace. The refractory pan is suspended from a high precision balance such that any change in the sample weight disturbs the balance equilibrium producing a proportional response to restore the equilibrium by electronic compensation so as to avoid the motion of the pan when the sample weight changes. Roberval type balance operates on the unique mechanism that allows high precision measurements and prevents sensitivity changes from factors like a thermal expansion.

Differential scanning calorimetry (DSC) is a technique that measures the change in the heat flow rate difference to the sample and the reference when subjected to a controlled temperature change. Thermal changes that do not comprise of the mass changes are represented in this technique. Similar to a DTA, DSC helps in determining the temperature of the phase transitions like melting point, the onset of oxidation and heat capacities, evaporation temperature, crystallization, etc. DSC profile gives the behavior of heat flux concerning time or temperature and hence, can be used to calculate the enthalpy, specific heat, etc. and is known to be more sensitive than a DTA. In DSC analysis a constant mass during the measurement of enthalpy change is desired.

Thermal analysis (TG and DSC) of samples powders was carried out using simultaneous TG-DSC (Mettler Toledo) thermal analyzer in the temperature range 30–1000 °C with a heating rate of 10 °C/min in a nitrogen atmosphere.



Figure 2.2 Experimental set-up of TG/DSC (Mettler Toledo, Germany)

2.3.2 X-Ray Diffraction (XRD)

X-Ray diffraction is a powerful characterization technique used for detailed structural analysis. The atomic arrangement of the structure can be deduced from the XRD patterns as the diffraction plane spacing (d) is of the order of X-Ray wavelength (λ), where the various orders (n) of reflection occur at precise values of diffraction angle (θ) satisfying the Bragg equation given by [Scott; Willard et al., 1986; Goodhew et al., 2001; Cullity, 1956];

$$2d_{hkl}\sin\theta = n\lambda \quad (2.1)$$

Advantages associated with these techniques are as follows

- (1) The XRD pattern acts as a blueprint of the substance under consideration.

(2) Each component in a mixture produces its characteristic pattern irrespective of the other component.

(3) Both qualitative (e.g., compound, structure, etc.) and quantitative (e.g., crystal size, d-spacing, lattice parameter, etc.) analysis of the substance can be achieved.

XRD characterization in the current work was carried out using Rigaku Miniflex II to confirm the formation of barium titanate, identify the phase formed, determine the crystallite size and lattice parameters. The measurement was carried out using a Cu-K' ($\lambda = 1.5405 \text{ \AA}$) X-Ray beam with a θ : the 2θ motion of the sample and the detector maintaining a step size of 0.02° at a scan rate of $2^\circ/\text{min}$. On the basis of XRD line broadening at half maxima of the maximum intensity diffraction peak, crystallite size (t) was estimated using the Debye-Scherrer formula,

$$t = \frac{0.9\lambda}{\beta \cos\theta} \quad (2.2)$$

Where λ is the wavelength of the target, β is the full width at half maxima (FWHM) in radians of the sample analyzed and θ is the Bragg angle.



Figure 2.3 X-ray diffraction pattern (XRD) set-up (Rigaku Miniflex II, Japan)

2.3.3 Density and Porosity Measurements

The bulk density (d_b) of the samples obtained using Archimedes' principle. Theoretical density (d_{th}) of the samples was calculated from the molecular weight of the samples and lattice parameters. The % porosity was calculated using the formula:

$$\% \text{ porosity} = \left[\frac{(d_{th} - d_b)}{d_{th}} \right] \times 100 \quad (2.3)$$

2.3.4 Fourier Transform Infrared (FTIR) Spectroscopy

Fourier transform infrared spectroscopy is a technique by which the chemical analysis of a material can be made as it studies the interaction of infrared light with matter. Above absolute zero, all universal objects radiate infrared radiation which can be absorbed by any matter on illumination. This absorption of the infrared radiation causes the chemical bond in the absorbing material to vibrate. Chemical structural fragments known as the functional groups (e.g., C-O group, OH group, C-H group, etc.) within molecules regardless of the molecular structure absorb

infrared radiation in the same wave number range which helps in identifying the molecules. The energy associated with infrared radiation is small and only induces a transition between the vibrational and the rotational energy levels of a molecule. Absorption of infrared radiation causes bond deformation by either stretching or bending of the functional group at quantized frequencies.

In the current study FTIR spectrophotometer FTIR- 8400S, SHIMADZU was employed in the transmittance mode from $400 - 4000\text{cm}^{-1}$. The final scan was recorded by averaging 100 scans at a resolution of 8.0 to obtain the FTIR profiles.



Figure 2.4 Experimental set-up FTIR spectrophotometer FTIR- 8400S, Shimadzu

2.3.5 Raman spectroscopy

Raman spectroscopy is an appropriate tool to get more insight into the local distortion, disorder and the strain present in the system because the vibrational spectrum has shorter characteristic length scale than required for the diffraction experiment. Raman scattering is also a useful tool to study the dynamics of the structure by analyzing the characteristics modes associated with nanoregions. The selection rules are very sensitive to the local and global symmetries.

In crystalline solids, the Raman Effect deals with phonons, instead of molecular vibrations. The fundamental requirement of a phonon to be a Raman active is that the first derivative of the polarizability concerning the normal vibrational coordinate has a zero value. A phonon can be active only in the crystals with no center of inversion.

Raman spectra are usually plotted in the intensity versus the difference in wave number between the incident beam and the scattered beam, and the peaks are in corresponding to the phonon frequency. Due to small wave vector of the optical phonons, the phonon involved in the Raman scattering of crystalline solids have (from the wave vector conservation law) a very small momentum compared with the Brillouin zone. So only the zone-centered phonons participate in Raman scattering.



Figure 2.5 Experimental set-up of Raman spectrometer

2.3.6 Transmission Electron Microscopy (TEM)

TEM is a technique in which electrons generated by an electron source penetrate a thin specimen (0.5"m or less) that are then imaged by specific lenses on a fluorescent screen or in the modern instruments by charge-coupled device (CCD) camera. In early TEMs gas discharge was used as the source of electrons which was then replaced by a V-shaped filament made from tungsten wire which when heated in vacuum emits electrons. The emitted electrons are accelerated by applying high voltage generated by electromagnetic lenses. Higher energy electrons resulting from higher accelerating voltage in the gun can penetrate comparatively thicker specimens which could otherwise not be imaged as the electrons would be stopped. The entire electron path from gun to the camera is maintained under vacuum so as to avoid scattering and absorption of electrons by the air molecules. TEM has been invaluable as it was capable of giving information about the structure of materials such as dislocations that validated some proposed theories. However, one limitation of producing a thin specimen for TEM analysis acts

as a constraint. This resulted in the study of developing electron microscopes capable of examining relatively thick specimens.



Figure 2.6 Experimental set-up of Transmission Electron Microscopy (TEM)

2.3.7 Scanning Electron Microscopy (SEM), Energy Dispersive Spectroscopy (EDS)

SEM is a technique in which the sample surface is scanned and analyzed when the electrons generated with an electron gun are irradiated over the sample. The SEM operates in two modes, namely; the secondary electron mode and the backscattered electron mode. In the secondary mode, the operation takes place when the high energy primary (i.e., incident) electron undergoes small angle scattering ($< 90^\circ$) which after irradiation re-emerges from the sample surface. However, in the backscattered mode, the high energy primary electron undergoes multiple elastic large angle scattering ($> 90^\circ$) within the specimen before re-emerging from the sample surface after irradiation. The energy from the secondary electron is less than that of the backscattered electron which has energy close to that of the primary electron. Backscattered electrons are rich in surface sensitive information due to which is highly important to the SEM users].

Energy dispersive spectroscopy is a semi-qualitative technique used in identifying and quantifying the elemental composition of a sample. On irradiating the sample with an electron beam in techniques like SEM, the atom in the sample radiates characteristic X-rays. These X-rays can be detected by the detector where the electron-hole pair is created using an energy dispersive spectrometer. This change having an energy proportional to the incoming X-ray is amplified and correlated to the atoms element according to its energy. However, this technique has a relatively poor energy resolution and is unable to detect lighter elements below sodium ($Z = 11$).

SEM analysis was carried out using two different instruments; this pellet was fractured and freshly fractured surfaces are gold coated using sputtering coating unit (Quorum Q150reS) as shown in Figure 2.7 (a) below. Scanning electron micrograph (Zeiss Evo18 Research Smartsem s/W), Figure 2.7 (b), of the samples were recorded at a different magnification of different regions at CIFIC, IIT (BHU).

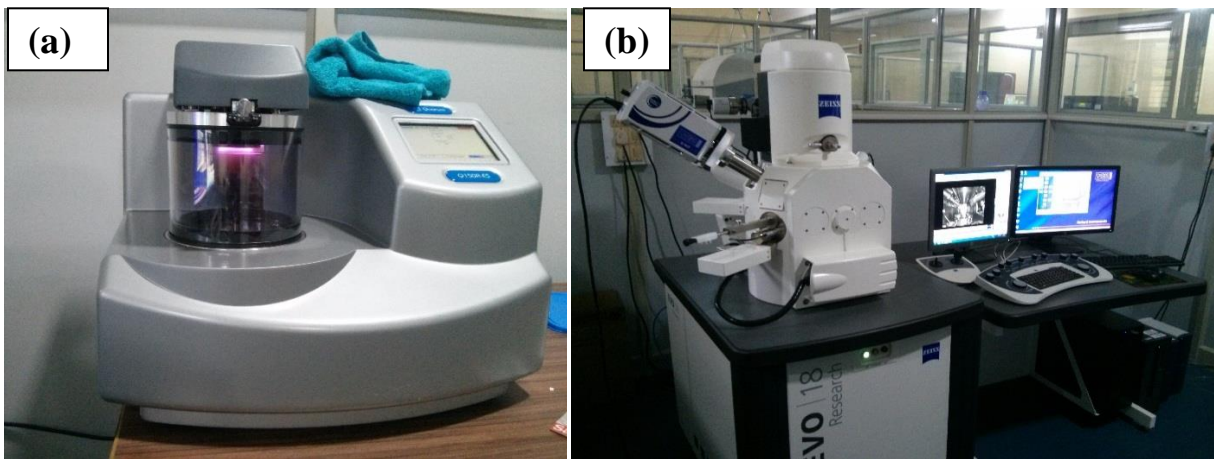


Figure 2.7 Experimental set-up of (a) Sputtering coating unit (Quorum Q150res) (b) Scanning electron micrograph (Zeiss Evo18 Research Smartsem S/W)

2.3.8 Dielectric Measurements

The electrical parameter used in characterizing electronic circuits, components and materials is its impedance [Barsoukov and Macdonald, 2005; Lei, 2006]. The basic elements comprise of inductance (L), capacitance (C) and resistance (R). By employing LCR meters and measuring the current flow through the material under study, all impedance parameters can be calculated. Thus, impedance spectroscopy is a technique in which the dielectric properties as a function of temperature, frequency and time are measured. The measured dielectric constant (property) of material is directly proportional to the capacitance of the material. The dielectric properties give an insight into the capacitive and conductive properties of the insulating material. The capacitive and conductive properties determine the materials capability to store electric charge and the motion of these charges within the material respectively. Phase transitions can also be identified using this technique. The dielectric constant of the material is related to its capacitance as

$$\epsilon_r = \frac{Cd}{\epsilon_0 A} \quad (2.4)$$

Where, ϵ_r is the dielectric constant, C the capacitance of the material, d the thickness of the pellet, ϵ_0 the permittivity of free space and A the area of the material.

The electrical properties of the sample pellet were observed by the dielectric measurement using a computer-controlled LCR meter (Wayne Kerr 6500 P, U.K.) at an ac signal of 1.0V. The measurements were made in the air in the temperature range -100 to 200 °C at different frequencies in the range 50 Hz to 2 MHz.



Figure 2.8 Computer-controlled LCR meter Set-up (Wayne Kerr 6500 P, U.K.)

2.3.9 Hysteresis loop

For hysteresis loop measurements, samples thickness- 0.5mm and diameter-12mm sliced using a diamond cutter (BUEHLER, ISOMET, LOW-SPEED SAW). Sliced pellets were polished in a similar way as the samples for dielectric measurements. Polished samples were electrode using Ag paint and cured at 700⁰C for 30Mint. Ferroelectric hysteresis (P-E) loops at room temperature for all the modified BT samples were recorded using an Automatic PE Loop Tracer of M/S AR Imagetronics. The system consists of a PC, Software, a programmable voltage source (up to 5kV) and Silicon oil bath. The measurement is based on modified Sawyer-Tower circuit, shown in Figure 2.9, operating at 50 Hz. For measurement, the specimen is kept in a spring-loaded jig and immersed in silicon oil. The loop is recorded by the system and the software computes all the parameters, e.g., Ps, Pr, and Ec. Software has the facility of cycling and averaging of the data points.

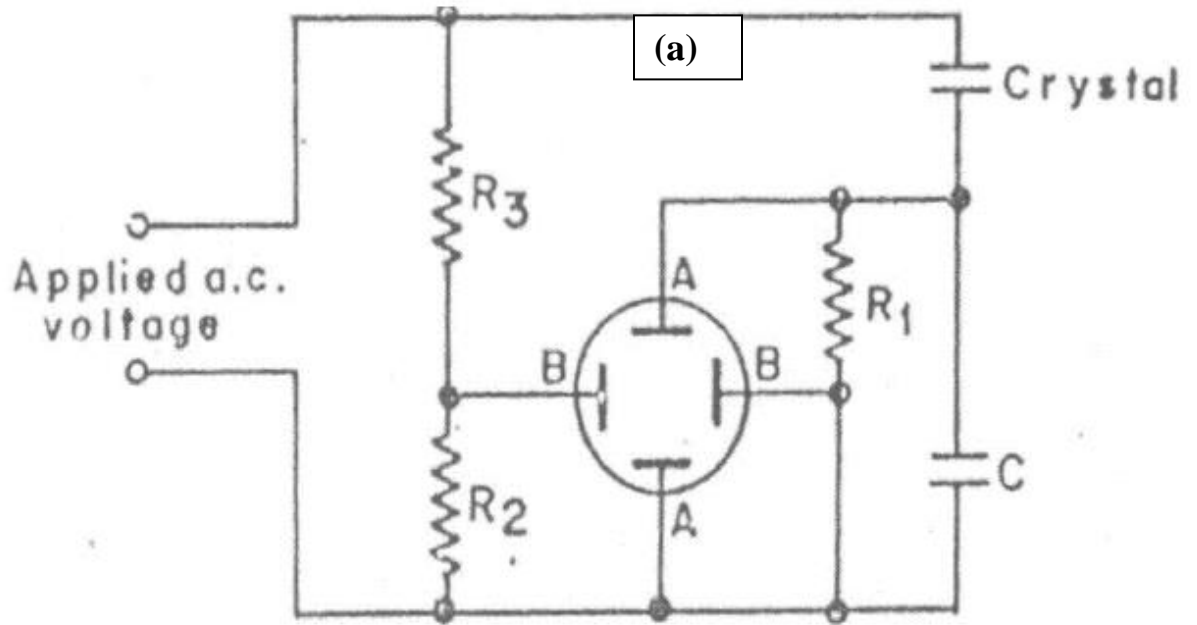


Figure 2.9 (a) Modified Sawyer-Tower Circuit for P-E measurements for bulk samples (b) P-E loop tracer setup (Marine, India)

2.3.10 Impedance Measurements and AC conductivity

Complex plane impedance spectroscopy is considered to be a promising non-destructive testing method for analyzing the electrical processes occurring in a compound on the application of ac. signal as input perturbation. Using this technique one can measure resistance due to grain interiors, grain boundaries and electrode independently. The equivalent electrical circuit shown below is widely used to fit impedance data of polycrystalline materials.

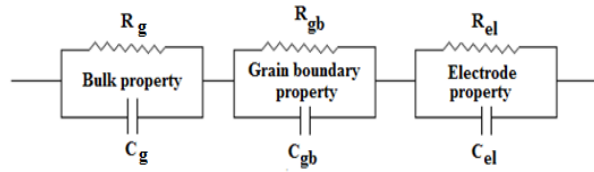


Figure 2.10 Equivalent circuit diagram for polycrystalline ceramic material

$$Z = Z' - jZ'' = (1/R_g + j\omega C_g)^{-1} + (1/R_{gb} + j\omega C_{gb})^{-1} + (1/R_{el} + j\omega C_{el})^{-1} \quad (2.5)$$

$$Z' = [(R_g)/(1+\omega^2 C_g^2 R_g^2) + (R_{gb})/(1+\omega^2 C_{gb}^2 R_{gb}^2) + (R_{el})/(1+\omega^2 C_{el}^2 R_{el}^2)] \quad (2.6)$$

$$Z'' = [(\omega R_g^2 C_g)/(1+\omega^2 C_g^2 R_g^2) + (\omega R_{gb}^2 C_{gb})/(1+\omega^2 C_{gb}^2 R_{gb}^2) + (\omega R_{el}^2 C_{el})/(1+\omega^2 C_{el}^2 R_{el}^2)] \quad (2.7)$$

Thus complex plane impedance plots (Z' vs. Z'') of materials exhibit an arc at high frequency, the second arc at lower frequencies, third arc at even lower frequencies. In complex plane impedance plot, ideal semicircle, appears only when the contribution to this arc is having single relaxation time. Total dc conductivity (σ_{dc}) was calculated using relation $\sigma_{dc} = (1/R_t) \cdot (t/A)$ where $R_t(R_g + R_{gb})$, where R_g and R_{gb} are grain and grain boundaries respectively) is total resistance, t is the thickness, and A is the area of the electrode deposited on the sample. Johnscher's attempted to explain the behavior of ac conductivity using the following universal power law:

$$\sigma = \sigma_{dc} [1 + (\frac{\omega}{\omega_H})^n] \quad (2.8)$$

Where, σ_{dc} = dc conductivity ω_H = hopping frequency, n is a frequency exponent in the range of $0 \leq n \leq 1$.